applied sciences

Article

Predictive and Explainable Artificial Intelligence for Weight Loss After Sleeve Gastrectomy: Insights from Wide and Deep Learning with Medical Image and Non-Image Data

Jaechan Park [1,†], Sungsoo Park [1,†], Kwang-Sig Lee [2,*] and Yeongkeun Kwon [1,*]

1 Department of Foregut Surgery, Korea University Anam Hospital, Seoul 02841, Republic of Korea; kei07099@naver.com (J.P.); kugspss@korea.ac.kr (S.P.)
2 AI Center, Korea University Anam Hospital, Seoul 02841, Republic of Korea
* Correspondence: ecophy@hanmail.net (K.-S.L.); kwon.yeongkeun@gmail.com (Y.K.)
† These authors contributed equally to this work.

Abstract: There has been no feasible approach for predicting weight loss after bariatric surgery. This study develops wide and deep learning (WAD), a predictive and explainable artificial intelligence for weight loss after sleeve gastrectomy with medical image and non-image data, such as electronic medical records (EMRs). Prospective data came from 42 patients with sleeve gastrectomy at a university hospital. They were followed for one year after surgery. The dependent variable consisted of three categories: minimal, moderate, and significant change groups, classified based on postoperative percentage total weight loss (%TWL) in body mass index. A pair of 100 images and their non-image data came from each patient, with 4200 pairs from 42 patients in total. A WAD model was trained and tested with 3200 and 1000 pairs, respectively. Here, the WAD model combined a convolutional neural network (CNN) for image data and a linear layer for non-image data (EMR). The study population included 42 patients, with a mean age of 36.6 years (standard deviation SD 11.0) and a female proportion of 58% (26/45). On average, %TWL was 19.1 (SD 2.8), 27.3 (SD 2.2), and 35.1 (SD 4.7) for the minimal, moderate, and significant change groups, respectively. The corresponding accuracy outcomes were 61%, 100%, and 75% for the minimal, moderate, and significant change groups (average 71%). When the minimal and moderate change groups were combined, the accuracy was 100% for the combined group and 75% for the significant change group, with an overall average accuracy of 88%. Baseline HOMA2-B, insulin, and vitamin B12 were major predictors of %TWL. The optimal region of interest for predicting %TWL was found to be the entire cross-section above the diaphragm. In conclusion, WAD is an effective predictive and explainable artificial intelligence for weight loss following sleeve gastrectomy with image and non-image data. The most important predictors of postoperative weight loss were identified as baseline HOMA2-B, insulin, and vitamin B12 levels, while the key region of interest (ROI) in abdominal CT imaging was the entire cross-section located above the diaphragm.

Keywords: body mass index; wide and deep learning; convolutional neural network

check for updates

Academic Editor: Pedro Couto

Received: 28 January 2025
Revised: 14 February 2025
Accepted: 21 February 2025
Published: 25 February 2025

Citation: Park, J.; Park, S.; Lee, K.-S.; Kwon, Y. Predictive and Explainable Artificial Intelligence for Weight Loss After Sleeve Gastrectomy: Insights from Wide and Deep Learning with Medical Image and Non-Image Data. *Appl. Sci.* **2025**, *15*, 2457. https://doi.org/10.3390/app15052457

1. Introduction

Bariatric surgery is currently the most successful and durable treatment for morbid obesity [1]. However, there exists wide variability in weight loss after bariatric surgery, and there exist few effective approaches for the prediction of postoperative weight loss, even though suboptimal weight loss after bariatric surgery is reported to be associated with the recurrence of obesity-related comorbidities and the deterioration of health-related life satisfaction [2]. Recent advances in artificial intelligence (AI) aid in the prognosis and treatment of diseases, including obesity [3]. This is welcome news. Predictive AI can help patients to adjust their expectations, given that 58% of them consider maximum postoperative weight loss to be the best outcome [4]. Furthermore, explainable AI can aid in identifying major predictors of postoperative weight loss, thereby delivering customized options for optimal surgery and follow-up interventions [5].

In fact, two important requirements for customized decision support systems for optimal surgery and follow-up interventions would be (1) that variables are easy to obtain and (2) that these variables can be analyzed in an integrated manner in case they involve multiple dimensions. A predictive AI with five convolutional layers, one dense layer, and two fully connected layers using preoperative computed tomography (CT) data was reported to achieve good performance for predicting surgical outcomes in abdominal wall construction, i.e., 81% [6]. However, previous studies on this topic used either preoperative abdominal image data or electronic medical record (EMR) data only [7–12]. Little literature is available on decision support systems for weight loss after sleeve gastrectomy with the combination of image and non-image data.

In this context, this study develops "wide and deep learning" (WAD), a predictive and explainable AI for weight loss one year after sleeve gastrectomy that uses abdominal CT data and EMR data. Specifically, WAD in this study predicts postoperative weight loss and identifies its major predictors and optimal regions of interest, so as to deliver effective customized decision support systems for optimal surgery and follow-up interventions.

2. Methods

2.1. Participants

This study utilized data from an ongoing original study conducted from 2020. The original study is a prospective, longitudinal, multi-omics study designed to ascertain the metabolic mechanisms of sleeve gastrectomy at a university hospital (Institutional Review Board Approval number: 2023AN0364). Patients were enrolled in the study if they met the following criteria: (1) body mass index (BMI) of 35 kg/m^2 or higher, (2) BMI of 30 kg/m^2 or higher in combination with at least one obesity-related comorbidity, or (3) aged between 20 and 60 years. Patients were excluded from participation if they had undergone bariatric surgery, other complex abdominal surgery, or had poorly controlled medical or psychiatric disorders (see Supplementary Table S1 for details of the eligibility criteria). Following enrolment in the study, all patients underwent nutritional evaluations. These evaluations included weight loss expectations, eating behaviors and patterns, physical activity habits, and psychosocial assessments. In order to achieve optimal weight loss following sleeve gastrectomy, a bariatric physician and a registered dietitian provided dietary and lifestyle recommendations. These recommendations included dietary principles, such as macro- and micro-nutrient compositions, carbohydrate counting, and advice regarding regular aerobic exercise. All patients initiated guideline-based micronutrient (vitamin and mineral) supplementation post-enrollment in the study [13].

Sleeve gastrectomies were performed laparoscopically by a single bariatric surgeon and involved a gastric volume reduction of 80% to 85% using a 30-French bougie to perform stomach resections beginning 3 cm from the pylorus and terminating at the angle of His. Postoperatively, patients received education via a protocol-driven staged meal progression. If tolerable, a low-sugar clear liquid meal was initiated within 24 h after sleeve gastrectomy, and soft and regular diets were recommended to begin at three to four weeks and nine weeks, respectively. It was recommended that patients consume 50 g of protein per day, with the option of up to 1.5 g of protein per kilogram of ideal body weight, via oral supplementation. In the initial four weeks following the procedure, patients were encouraged to engage in physical activity, commencing with gentle walks and progressively augmenting their speed to a level that they could comfortably sustain. Patients were instructed to walk for a minimum of 150 min per week. In the 5–26 weeks following surgery, the patients' total walking time was increased to a minimum of 200 min per week and at least four days per week. Additionally, patients were asked to perform three ≥20 min strength exercise sessions, including shoulder and hip strengthening exercises, ≥3 days per week. The intensity of these exercises was measured using the Borg Scale [14], with a perceived exertion rating between 12 and 14 indicating a moderate level of physical exertion. All participants were subjected to follow-up procedures at two-week intervals, which incorporated telephone and text message communication, with the objective of confirming adherence to the stipulated nutritional and exercise recommendations.

2.2. Variables

The dependent (or outcome) variable was categorized into three groups based on the percentage of total body weight loss (%TWL) after sleeve gastrectomy: the upper 1/3, with the biggest weight loss (significant change group), the lower 1/3, with the smallest weight loss (minimal change group), and the middle 1/3 (moderate change group). The %TWL was calculated as the weight reduction one year after bariatric surgery, divided by the preoperative weight. The following independent (or predictor) variables were included in this study: (1) baseline information; (2) laboratory data; and (3) bioelectrical impedance analysis (BIA). Among the laboratory data, HOMA2 (Homeostasis Model Assessment 2) is calculated based on fasting glucose, fasting insulin, and C-peptide levels to assess insulin resistance and insulin secretion capacity. Specifically, HOMA-2S evaluates the responsiveness of cells and tissues to insulin, HOMA2-IR indicates the level of insulin resistance, and HOMA-2B assesses the insulin secretion function of pancreatic beta cells. Bioelectrical impedance analysis (BIA) estimates body composition by measuring impedance using a low-level electrical current. In this study, fat mass and skeletal muscle mass were measured as variables through BIA.

2.3. Analysis

Descriptive statistics are presented as proportions for categorical variables and as averages with standard deviations (SDs) for continuous variables. Patients' characteristics at baseline and three postoperative periods were compared based on a paired t-test. A two-sided p-value of <0.05 was considered statistically significant. The source of data was abdominal CT images and 32 clinical observation data points from 42 sleeve gastrectomy patients at baseline. Among these 4200 image–observation data pairs, 3200 and 1000 were used for training and test sets, respectively. Figure 1 shows the flow chart for WAD. For the prediction of the three categories for BMI change, the WAD model was trained and tested: a convolutional neural network (CNN) processes the image data; a linear layer integrates the non-image data, which consists of clinical observation data derived from electronic medical records (EMRs). In the first stage, original images were used for training and testing the Stage-1 WAD. In the second stage, optimal regions of interest (ROIs) were found based on reinforcement learning (neural architecture search) for the Stage-1 WAD, and then these optimal ROIs were employed for training and testing the Stage-2 WAD. Here, neural architecture search denotes systematic selection for the width and height of the region of interest, which maximizes the performance of WAD.

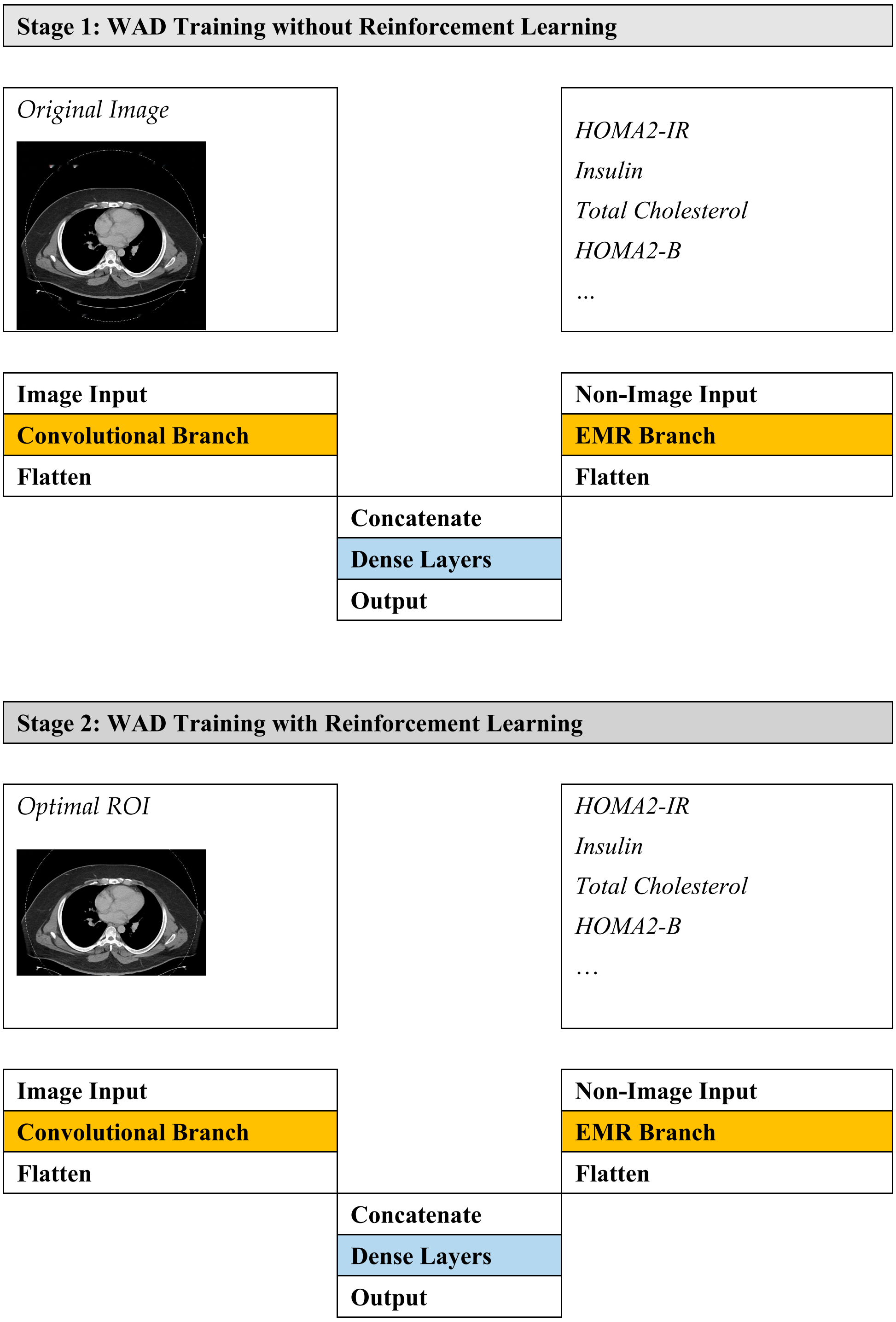

Figure 1. Flow chart for the wide and deep model. Legend: For the prediction of three categories for body mass index change, the wide and deep (WAD) model was trained and tested: a convolutional neural network (CNN) processes the image data; a linear layer integrates the non-image data, which consist of clinical observation data derived from electronic medical records (EMRs). In the first stage, original images were used for training and testing the Stage-1 WAD. In the second stage, optimal regions of interest (ROIs) were found based on reinforcement learning for the Stage-1 WAD, and then these optimal ROIs were employed for training and testing the Stage-2 WAD.

The CNN branch, which accepts the image input of the shape (300, 300, and 3), consists of six convolutional blocks, as described in Figure 2. Each of the first three convolutional blocks contains the following: (1) a convolutional layer with 32 filters of size 4 and the activation function of the rectified linear unit; (2) a max pooling layer of size 2. Each of the second three convolutional blocks includes the following: (1) a convolutional layer with 16 filters of size 4 and the activation function of the rectified linear unit; (2) a max pooling layer of size 2. The output from the last layer of the CNN branch and the linear layer containing clinical observation data (with a shape of 32) are both flattened, then concatenated, and subsequently followed by three dense layers. The first or second dense layer has 10 output neurons, with the activation function of the rectified linear unit. The third dense layer has 4 output neurons, with the activation function of sigmoid. Stata12 (Stata Corp., College Station, TX, USA, 2011), Keras 2.3.0 (Francois Chollet, GitHub, San Francisco, CA, USA, 2015), and the Lenovo ST650 V2 GPU Server were employed for the analysis during 1 January 2024–30 April 2024.

Layer	Hyper-Parameter		
Input[1]	300	300	3
Convolutional Branch			
Convolution[2]	32	4	RELU
Max Pooling[3]	2		
Convolution	32	4	RELU
Max Pooling	2		
Convolution	32	4	RELU
Max Pooling	2		
Convolution	16	4	RELU
Max Pooling	2		
Convolution	16	4	RELU
Max Pooling	2		
Convolution	16	4	RELU
Max Pooling	2		
Flatten			
Dense Layers			
Dense[4]	10		RELU
Dense	10		RELU
Dense[5]	4		SIGM
Output			

Figure 2. Convolutional neural network branch. Note: [1] the image input of the shape (300, 300, and 3); [2] the convolutional layer with 32 filters of size 4 and the activation function of the rectified linear unit; [3] the max pooling layer of size 2; [4] the dense layer with 10 output neurons and the activation function of the rectified linear unit; [5] the dense layer with 4 output neurons and the activation function of sigmoid.

3. Results

3.1. Participant Characteristics

The average weight after sleeve gastrectomy over all groups was 82.3 kg (standard deviation SD 15.1). The average percentage of total weight loss (%TWL) one year after sleeve gastrectomy over all groups was 26.8% (SD 7.3). The average %TWL of the minimal change group was 19.1% (SD 2.8), while its moderate change group and significant change group counterparts were 27.3% (SD 2.2) and 35.1% (SD 4.7), respectively. Based on the results of the t-test, there was a statistically significant weight difference between pre-surgery and post-surgery in each group ($p < 0.010$, $p < 0.001$, and $p < 0.001$) (Figure 3). The corresponding averages of the 42 study participants were as follows: (1) 36.6 years (SD 11.02) for age, 112.4 kg (SD 19.5) for weight, and 39.8 kg/m^2 (SD 4.9) for BMI; (2) 152.3% (SD 66.1) for HOMA2-B, 45.9% (SD 50.0) for HOMA2-S, and 3.2 (SD 1.5) for HOMA2-IR; and

(3) 86.7 µg/d (SD 41.2) for iron and 672.7 pg/mL (SD 274.0) for vitamin B12. The respective proportions were 58% for female status, 36% for type 2 diabetes, 51% for dyslipidemia, and 22% for depression (Table 1).

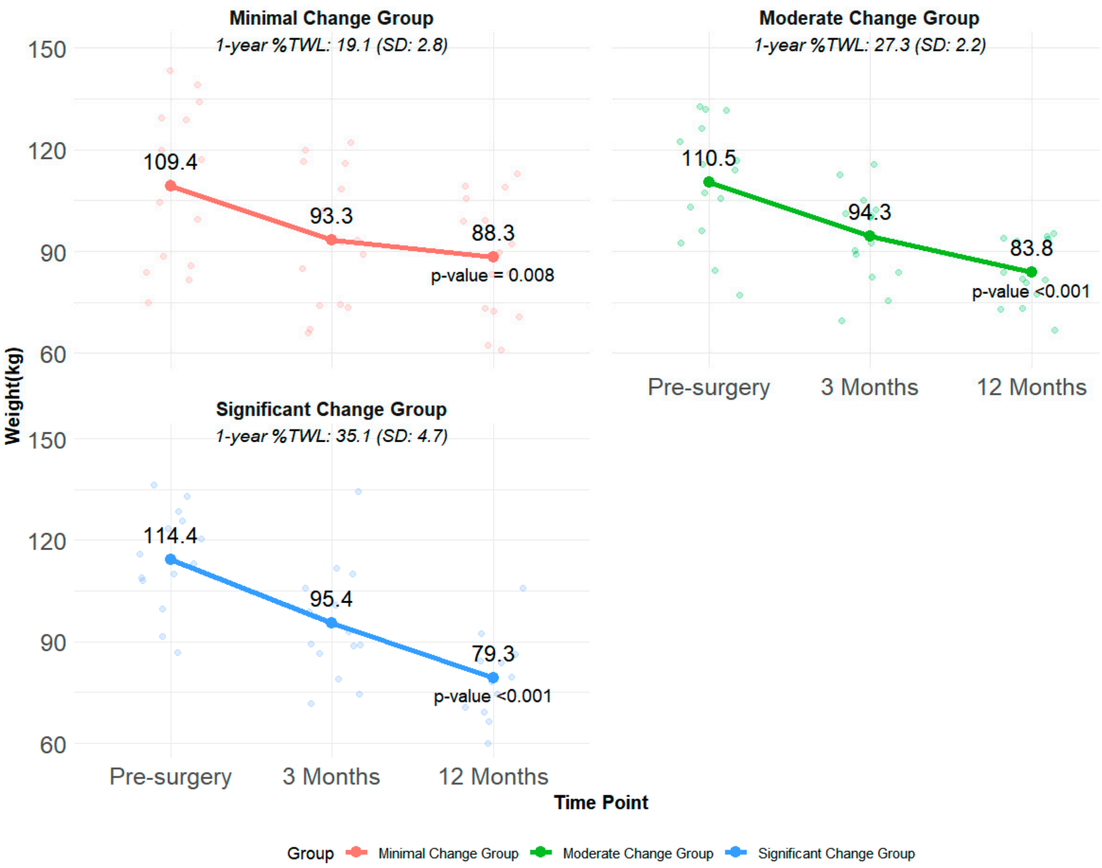

Figure 3. Weight loss after sleeve gastrectomy. Legend: based on the results of t-test, there was a statistically significant weight difference between pre-surgery and post-surgery in each group ($p < 0.010$, $p < 0.001$, and $p < 0.001$).

Table 1. Baseline characteristics.

Variables	Values (n = 45)
Age, year	36.6 (11.0)
Female, n (%)	26 (58)
Weight, kg	112.4 (19.5)
Body mass index, kg/m^2	39.8 (4.9)
Skeletal muscle mass, kg	34.0 (7.0)
Fat mass, kg	53.0 (12.5)
Waist circumference, cm	125.6 (14.9)
Hemoglobin, g/dL	14.4 (1.8)
Aspartate transaminase, IU/L	47.3 (31.0)
Alanine transaminase, IU/L	67.7 (60.9)
Fasting plasma glucose, mg/dL	109.4 (13.1)
Fasting plasma insulin, mg/dL	24.8 (12.7)
HOMA2-B (%)	152.3 (66.1)

Table 1. *Cont.*

Variables	Values (n = 45)
HOMA2-S (%)	45.9 (50.0)
HOMA2-IR	3.2 (1.5)
HbA1c, %	6.3 (1.1)
C-reactive protein, ng/mL	5.2 (6.5)
Uric acid, mg/dL	6.2 (1.8)
Total cholesterol, mg/dL	176.0 (43.6)
Triglyceride, mg/dL	146.0 (63.3)
High density lipoprotein cholesterol, mg/dL	46.7 (10.4)
Low density lipoprotein cholesterol, mg/dL	106.7 (39.8)
Iron, µg/dL	86.7 (41.2)
Vitamin B_{12}, pg/mL	672.7 (274.0)
Systolic blood pressure, mmHg	142.1 (13.8)
Hypertension, n (%)	33 (73)
Type 2 diabetes, n (%)	16 (36)
Dyslipidemia, n (%)	23 (51)
Depression, n (%)	10 (22)

Values are given as mean ± standard deviation.

3.2. Model Performance and Variable Importance

During 600 epochs, the test set loss of WAD registered a steady fall from 23 to 13 (Figure 4). The accuracy results were 61%, 100%, and 75% for the minimal, moderate, and significant change groups, correspondingly (average 71%). With the minimal and moderate change groups being combined, the accuracy outcomes were 100% and 75% for the combined and significant groups, respectively (average 88%) (Table 2). Here, accuracy means "accuracy for a class", i.e., predicted observations over actual observations for a class, namely, 0, 1, or 2. This becomes specificity (for a class of "0") or sensitivity (for a class of "1") in the case of binary prediction. Average accuracy is a simple form of the F1 score. Based on reinforcement learning (neural architecture search), the optimal region of interest for predicting weight loss was identified as the entire cross-section above the diaphragm, as shown in Figure 5. As explained above, neural architecture search represents systematic selection for the width and height of the region of interest, which maximizes the performance of WAD. This study identified baseline HOMA2-B, insulin, and vitamin B12 as the most important predictors of BMI change over one year. The importance of a predictor was calculated by the performance gap between the model without its permutation and the model with its permutation ("variable permutation importance"). Here, permutation refers to randomly shuffling the values of a particular variable so that it no longer contributes to the model's prediction process. For example, the importance of HOMA2-B, 0.1255, indicates a performance difference between WD without its permutation and WD with its permutation. The permutation importance rankings of five predictors, HOMA2-B, insulin, vitamin B12, fast plasma glucose, alanine transaminase, and HOMA2-S, were similar in WD and RF, a popular machine learning model. Here, the terms WD and RF denote wide and deep learning and random forest, respectively (Table 3).

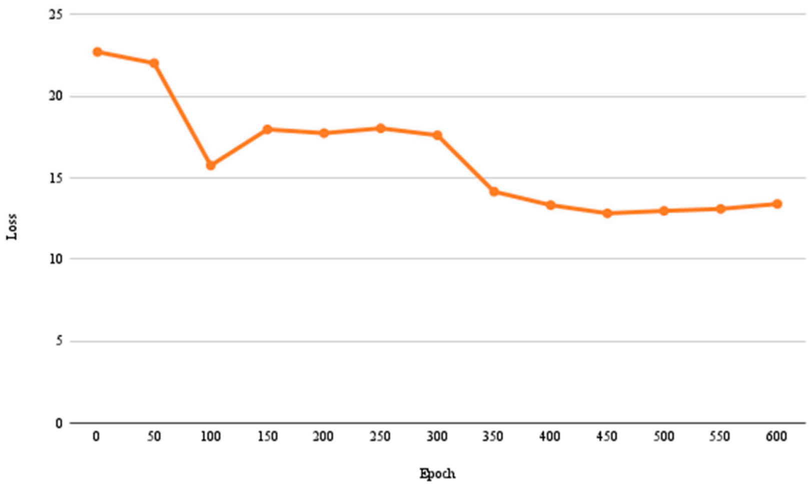

Figure 4. Test set loss of wide and deep learning during 600 epochs. Legend: during 600 epochs, the test set loss of wide and deep learning registered a steady fall from 23 to 13.

Table 2. Model performance. Legend: The accuracy results were 61%, 100%, and 75% for the minimal, moderate, and significant change groups, correspondingly (average 71%). When the minimal and moderate change groups were combined, the accuracy outcomes were 100% and 75% for the combined minimal and moderate group and significant change group, respectively (average 88%).

Accuracy	3-Class	2-Class
G1	0.61	
G2	1.00	1.00
G3	0.75	0.75
Total	0.71	0.88

Note: G1, minimal change group; G2, moderate change group; G3, significant change group.

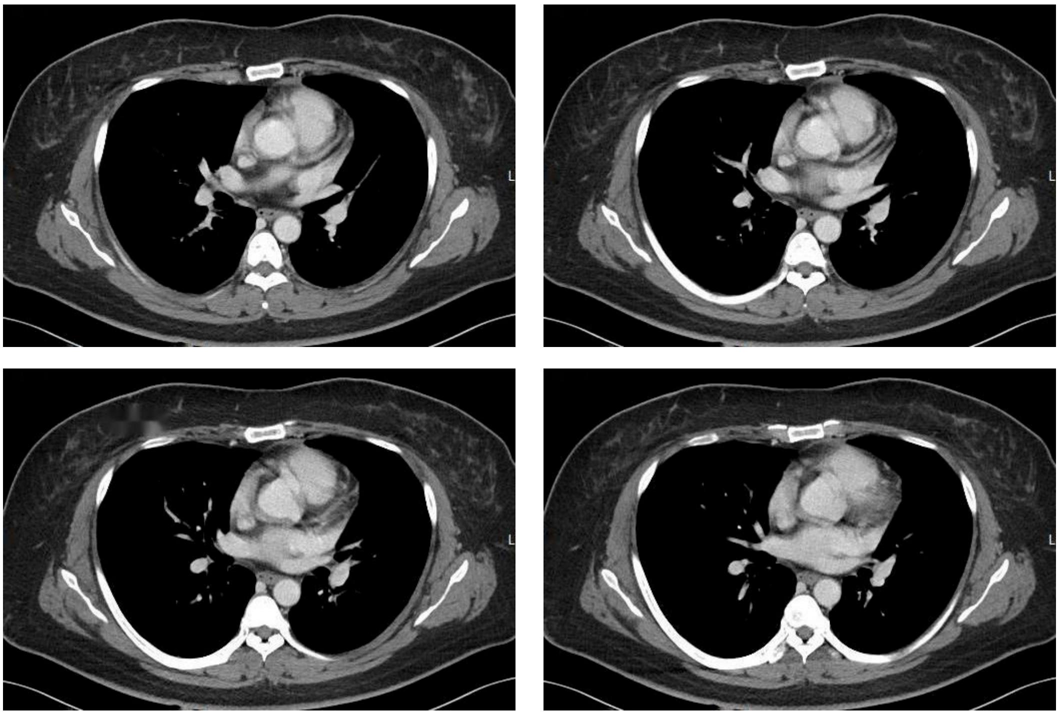

Figure 5. Optimal regions of interest based on reinforcement learning. Legend: analysis of abdominal CT images using reinforcement learning (neural architecture search) to identify the region of interest most associated with weight loss revealed that the entire cross-section at the above-diaphragm level was the most significant.

Table 3. Permutation importance. Legend: The importance of a predictor was calculated as the performance gap between the model without its permutation and the model with its permutation ("variable permutation importance"). For example, the importance of HOMA2-B, 0.1255, indicates a performance difference between wide and deep learning without its permutation and wide and deep learning with its permutation. The permutation importance rankings of five predictors, HOMA2-B, insulin, vitamin B12, fast plasma glucose, alanine transaminase, and HOMA2-S, were similar in WD and RF, a popular machine learning model. Here, the terms WD and RF denote wide and deep learning and random forest, respectively.

Variable	**WD**		**RF**	
	VI	*Rank*	*VI*	*Rank*
HOMA2-B	0.1255	4	0.1398	1
Insulin	0.1275	2	0.0770	2
Uric Acid	0.0020	8	0.0675	3
Vitamine B12	0.0387	5	0.0557	4
HOMA2-IR	0.1289	1	0.0473	5
SMM	0.0000	10	0.0453	6
Glucose	0.0059	6	0.0436	7
ALT	0.0054	7	0.0435	8
HOMA2-S	0.0010	9	0.0428	9
Total Cholesterol	0.1270	3	0.0364	10

Note: WD, wide and deep; RF, random forest; VI, variable importance; SMM, skeletal muscle mass.

4. Discussion

The prediction of weight loss following bariatric surgery remains a challenging task. A plethora of studies have sought to formulate models for the prediction of weight loss post-surgery. However, retrospective validation of these models has revealed that, while many demonstrated a statistically significant correlation with post-surgery weight, even the most accurate models could only explain 24% of the variation in weight loss [15]. Furthermore, the majority of models tended to overestimate outcomes. While some studies have employed machine learning techniques to identify variables influencing post-surgical weight loss [16], these have frequently been constrained by their reliance on simplistic factors such as height, weight, diabetes status, and diabetes duration.

This study presents the first endeavor to formulate a deep learning model that utilizes both imaging and non-imaging data to predict outcomes following sleeve gastrectomy. The model incorporates a comprehensive set of variables, encompassing not only basic characteristics such as height and weight, but also metrics of insulin resistance, blood pressure, and computed tomography (CT) imaging data. The integration of these diverse variables has yielded a novel perspective on predicting weight loss after bariatric surgery. The findings of this study demonstrated that the model achieved a higher level of accuracy in predicting post-surgical weight loss compared to a previous study on a similar topic but with imaging data only [6] (88% vs. 81%). This accuracy gap remained intact for another study, which developed an artificial neural network on non-image data only with 17 variables [10] (88% vs. 70%). Of particular significance was the identification of insulin resistance and secretion markers (HOMA-IR, HOMA2-B, and insulin) as critical predictors of weight loss outcomes. Furthermore, this study identified that the most significant CT cross-sectional region associated with weight change prediction was the diaphragm-level section of the abdomen.

The findings of this study indicate that insulin resistance and secretion-related indicators—HOMA2-B, HOMA2-IR, and insulin—play pivotal roles in predicting post-surgery weight loss. Insulin resistance and the decline in beta cell function are central to the pathophysiology of type 2 diabetes mellitus (T2DM). The Homeostasis Model Assessment 2 (HOMA2) is a method that estimates insulin resistance (HOMA2-IR) and β-cell secretion capacity (HOMA2-B) using fasting plasma glucose (FPG) and fasting C-peptide levels. Given that HOMA2-IR reflects insulin resistance, it aligns with the influence of insulin levels on weight loss observed in our model. The significance of insulin resistance in weight regulation is further substantiated by several studies, which demonstrate that hyperinsulinemia or insulin resistance may potentially augment the probability of substantial weight reduction by up to threefold [17]. The underlying mechanism by which our findings were observed may be related to the role of insulin resistance in promoting weight gain. Insulin exerts its suppressive effect on lipolysis under typical conditions; however, in individuals with insulin resistance, the presence of hyperinsulinemia activates lipoprotein lipase on fat cell membranes and enhances the synthesis of fatty acid-binding proteins, thereby promoting the accumulation of free fatty acids (FFAs) within adipocytes [18]. Consequently, the development of insulin resistance can contribute to weight gain. Bariatric surgery has been shown to reduce both weight and insulin resistance [19]. The findings of this study suggest that patients with higher preoperative HOMA2-IR or basal insulin levels may experience more pronounced weight loss after surgery due to the greater reduction in insulin resistance postoperatively.

HOMA2-B is a metric that reflects the insulin secretion capacity of pancreatic β-cells. The findings of this study indicate a correlation between preoperative insulin secretion and postoperative weight change, which is consistent with the conclusions of several previous studies. Retrospective research has demonstrated a negative relationship between HOMA-B and the percentage of total body weight loss (TBWL) at 2, 3, and 4 years post-surgery [20]. Furthermore, a study comparing patients who achieved complete remission (CR) of type 2 diabetes mellitus (T2DM) after bariatric surgery with those who did not (non-CR) found that CR was associated with postoperative weight change, and preoperative HOMA2-B was a key predictor of remission [21]. One hypothesis to elucidate the association between preoperative β-cell function and postoperative weight loss is that patients with low insulin secretion before surgery may continue to experience limited insulin secretion postoperatively, even if insulin resistance improves [22]. Consequently, insufficient insulin secretion might limit the extent of weight loss [23], probably because of the lack of anabolic function of insulin. Another hypothesis is the normalization of adipokine secretion from adipocytes following weight loss. Adiponectin, a type of adipokine, plays a role in protecting pancreatic beta cells to maintain insulin secretion capacity [24,25]. Adiponectin activates AMP-activated protein kinase (AMPK), increasing energy expenditure and promoting the oxidation of glucose and fatty acids, thereby facilitating weight loss [26]. Individuals with reduced insulin secretion capacity may have decreased adiponectin levels. It has been demonstrated that weight reduction can lead to the normalization of adiponectin secretion [27,28]. Consequently, individuals with impaired insulin secretion capacity may experience enhanced weight loss as a consequence of the normalization of adiponectin levels.

This study identified vitamin B12 as a significant predictor of postoperative weight change. Vitamin B12, a water-soluble vitamin, is obtained through dietary intake and synthesized by the gut microbiome. It plays essential roles in cellular metabolism, DNA synthesis, epigenetic regulation, and mitochondrial metabolism. The findings of this study agree with those of previous research, which demonstrated an inverse relationship between B12 levels and BMI [29] and between B12 levels and adiposity in children [30]. According to another study [31], maternal rats fed a diet deficient in B12 not only exhibited increases in body fat and alterations in their lipid profile but also transmitted these effects to their offspring, which demonstrated significantly elevated visceral fat at three months and developed dyslipidemia by twelve months of age. The underlying mechanism by which B12 levels influence weight changes may involve processes related to lipid metabolism and alterations in the microbiome. The existing literature has also demonstrated that in B12-deficient adipocytes, cholesterol biosynthesis-related genes undergo hypomethylation, leading to increased expression and cholesterol synthesis [32]. Furthermore, an observation that microbially produced B12 enhances liver lipid metabolism and reduces lipogenesis suggests a potential role for B12 in weight loss mechanisms [33].

This study also identified the superdiaphragmatic cross-section as a key region of interest (ROI) in abdominal CT imaging for predicting weight loss. Various intra-abdominal organs were examined as potential ROIs, including the liver, pancreas, and small intestine. However, the above-diaphragm-level cross-section consistently emerged as the most relevant ROI. This finding suggests that subcutaneous fat at this level plays a crucial role in predicting postoperative weight change. This result aligns with prior studies [34] that reported a lower CT radiodensity of abdominal subcutaneous fat in obese individuals compared to non-obese individuals. Additionally, these studies identified post-surgical changes in radiodensity as being associated with clinical outcomes. In addition, research on patients with liver cirrhosis [35] found that subcutaneous fat radiodensity was associated with mortality. Histological analysis revealed correlations between fat tissue characteristics and clinical outcomes, suggesting that similar mechanisms could potentially play a role in predicting postoperative weight loss in our study.

This study has its limitations. First, while the identification of key variables—HOMA2-B, HOMA2-IR, insulin, and the above-diaphragm-level cross-section—was achieved, the determination of whether these factors have positive or negative effects on weight loss, as well as the quantification of their effect sizes, remains elusive. To further elucidate these relationships, additional research employing advanced interpretability techniques for deep learning models is imperative. Secondly, the development of the model was constrained by the utilization of data from 42 patients. To ensure the model's generalizability, future research should validate it across a more extensive and diverse patient population. Thirdly, this study used training and test sets from an internal source only. Employing external validation sets is expected to improve the performance and validity of WAD. Fourthly, while we hypothesized that subcutaneous fat located above the diaphragm level plays a role in weight loss, more precise segmentation of organs and anatomical structures through imaging analysis is needed to confirm this interpretation.

5. Conclusions

The present study underscores the significance of insulin secretion markers—HOMA2-B, HOMA2-IR, and insulin—as well as the superdiaphragmatic cross-section in predicting weight loss following sleeve gastrectomy. This research demonstrates the potential of machine learning to identify critical variables from a diverse range of data sources, including imaging and clinical metrics. The development of predictive models for weight change after sleeve gastrectomy holds promise in supporting decision-making for patients considering bariatric surgery, helping them make more informed choices and improving personalized postoperative care. Further studies are needed to determine the direction of effect for each variable and to validate the findings in a more diverse patient population.

Supplementary Materials: The following supporting information can be downloaded at: https://www.mdpi.com/article/10.3390/app15052457/s1, Table S1: Inclusion and exclusion criteria.

Author Contributions: S.P., K.-S.L. and Y.K. designed the study. J.P., K.-S.L. and Y.K. collected, analyzed, and interpreted the data. J.P., S.P., K.-S.L. and Y.K. wrote and reviewed the manuscript. J.P.,

S.P., K.-S.L. and Y.K. approved the final version of the manuscript. All authors have read and agreed to the published version of the manuscript.

Funding: This work was supported by a grant of Korea University Anam Hospital (Seoul, Republic of Korea) (Y.K.) and the Korea Health Industry Development Institute grant (HI22C1302 (Korea Health Technology R&D Project)) funded by the Ministry of Health and Welfare of South Korea (K.-S.L.). The funder had no role in the design of the study, in the collection, analysis and interpretation of the data, or the writing and review of the manuscript.

Institutional Review Board Statement: This retrospective study was approved by the Institutional Review Board of Korea University Anam Hospital on 17 August 2023 (2023AN0364). All methods were performed in accordance with the relevant guidelines and regulations.

Informed Consent Statement: Written informed consent was obtained from all patients.

Data Availability Statement: The original contributions presented in this study are included in the article and Supplementary Material. Further inquiries can be directed to the corresponding authors.

Conflicts of Interest: The authors declare no conflicts of interest.

References

1. Pipek, L.Z.; Moraes, W.A.F.; Nobetani, R.M.; Cortez, V.S.; Condi, A.S.; Taba, J.V.; Nascimento, R.F.V.; Suzuki, M.O.; do Nascimento, F.S.; de Mattos, V.C.; et al. Surgery is associated with better long-term outcomes than pharmacological treatment for obesity: A systematic review and meta-analysis. *Sci. Rep.* **2024**, *14*, 9521. [CrossRef] [PubMed]
2. Belligoli, A.; Bettini, S.; Segato, G.; Busetto, L. Predicting responses to bariatric and metabolic surgery. *Curr. Obes. Rep.* **2020**, *9*, 373–379. [CrossRef] [PubMed]
3. An, R.; Shen, J.; Xiao, Y. Applications of artificial intelligence to obesity research: Scoping review of methodologies. *J. Med. Internet Res.* **2022**, *24*, e40589. [CrossRef]
4. Weinstein, A.L.; Marascalchi, B.J.; Spiegel, M.A.; Saunders, J.K.; Fagerlin, A.; Parikh, M. Patient preferences and bariatric surgery procedure selection; the need for shared decision-making. *Obes. Surg.* **2014**, *24*, 1933–1939. [CrossRef] [PubMed]
5. Ochs, V.; Tobler, A.; Wolleb, J.; Bieder, F.; Saad, B.; Enodien, B.; Fischer, L.E.; Honaker, M.D.; Drews, S.; Rosenblum, I.; et al. Development of predictive model for predicting postoperative BMI and optimize bariatric surgery: A single center pilot study. *Surg. Obes. Relat. Dis.* **2024**, *20*, 1234–1243. [CrossRef] [PubMed]
6. Elhage, S.A.; Deerenberg, E.B.; Ayuso, S.A.; Murphy, K.J.; Shao, J.M.; Kercher, K.W.; Smart, N.J.; Fischer, J.P.; Augenstein, V.A.; Colavita, P.D.; et al. Development and validation of image-based deep learning models to predict surgical complexity and complications in abdominal wall reconstruction. *JAMA Surg.* **2021**, *156*, 933–940. [CrossRef]
7. Shi, J.; Bao, G.; Hong, J.; Wang, S.; Chen, Y.; Zhao, S.; Gao, A.; Zhang, R.; Hu, J.; Yang, W.; et al. Deciphering CT texture features of human visceral fat to evaluate metabolic disorders and surgery-induced weight loss effects. *eBioMedicine* **2021**, *69*, 103471. [CrossRef]
8. Bellini, V.; Valente, M.; Turetti, M.; Del Rio, P.; Saturno, F.; Maffezzoni, M.; Bignami, E. Current Applications of Artificial Intelligence in Bariatric Surgery. *Obes. Surg.* **2022**, *32*, 2717–2733. [CrossRef]
9. Bektaş, M.; Reiber, B.M.; Pereira, J.C.; Burchell, G.L.; van der Peet, D.L. Artificial Intelligence in Bariatric Surgery: Current Status and Future Perspectives. *Obes. Surg.* **2022**, *32*, 2772–2783. [CrossRef]
10. Piaggi, P.; Lippi, C.; Fierabracci, P.; Maffei, M.; Calderone, A.; Mauri, M.; Anselmino, M.; Cassano, G.B.; Vitti, P.; Pinchera, A.; et al. Artificial neural networks in the outcome prediction of adjustable gastric banding in obese women. *PLoS ONE* **2010**, *5*, e13624. [CrossRef]
11. Lee, Y.C.; Lee, W.J.; Lee, T.S.; Lin, Y.C.; Wang, W.; Liew, P.L.; Huang, M.T.; Chien, C.W. Prediction of successful weight reduction after bariatric surgery by data mining technologies. *Obes. Surg.* **2007**, *17*, 1235–1241. [CrossRef] [PubMed]
12. Wise, E.S.; Hocking, K.M.; Kavic, S.M. Prediction of excess weight loss after laparoscopic Roux-en-Y gastric bypass: Data from an artificial neural network. *Surg. Endosc.* **2016**, *30*, 480–488. [CrossRef] [PubMed]
13. Quilliot, D.; Coupaye, M.; Ciangura, C.; Czernichow, S.; Sallé, A.; Gaborit, B.; Alligier, M.; Nguyen-Thi, P.L.; Dargent, J.; Msika, S.; et al. Recommendations for nutritional care after bariatric surgery: Recommendations for best practice and SOFFCO-MM/AFERO/SFNCM/expert consensus. *J. Visc. Surg.* **2021**, *158*, 51–61. [CrossRef]
14. Williams, N. The Borg Rating of Perceived Exertion (RPE) scale. *Occup. Med.* **2017**, *67*, 404–405. [CrossRef]
15. Karpińska, I.A.; Kulawik, J.; Pisarska-Adamczyk, M.; Wysocki, M.; Pędziwiatr, M.; Major, P. Is It Possible to Predict Weight Loss After Bariatric Surgery?—External Validation of Predictive Models. *Obes. Surg.* **2021**, *31*, 2994–3004. [CrossRef]

16. Saux, P.; Bauvin, P.; Raverdy, V.; Teigny, J.; Verkindt, H.; Soumphonphakdy, T.; Debert, M.; Jacobs, A.; Jacobs, D.; Monpellier, V.; et al. Development and validation of an interpretable machine learning-based calculator for predicting 5-year weight trajectories after bariatric surgery: A multinational retrospective cohort SOPHIA study. *Lancet Digit. Health* **2023**, *5*, e692–e702. [CrossRef]
17. Wedick, N.M.; Mayer-Davis, E.J.; Wingard, D.L.; Addy, C.L.; Barrett-Connor, E. Insulin resistance precedes weight loss in adults without diabetes: The Rancho Bernardo Study. *Am J Epidemiol* **2001**, *153*, 1199–1205. [CrossRef]
18. Sears, B.; Perry, M. The role of fatty acids in insulin resistance. *Lipids Health Dis.* **2015**, *14*, 121. [CrossRef]
19. Benaiges, D.; Le-Roux, J.A.F.; Pedro-Botet, J.; Chillarón, J.J.; Renard, M.; Parri, A.; Ramón, J.M.; Pera, M.; Goday, A. Sleeve gastrectomy and Roux-en-Y gastric bypass are equally effective in correcting insulin resistance. *Int. J. Surg.* **2013**, *11*, 309–313. [CrossRef]
20. Borges-Canha, M.; Neves, J.S.; Mendonca, F.; Silva, M.M.; Costa, C.; MCabral, P.; Guerreiro, V.; Lourenco, R.; Meira, P.; Salazar, D.; et al. Beta cell function as a baseline predictor of weight loss after bariatric surgery. *Front. Endocrinol.* **2021**, *12*, 714173. [CrossRef]
21. Souteiro, P.; Belo, S.; Neves, J.S.; Magalhães, D.; Silva, R.B.; Oliveira, S.C.; Costa, M.M.; Saavedra, A.; Oliveira, J.; Cunha, F.; et al. Preoperative beta cell function is predictive of diabetes remission after bariatric surgery. *Obes. Surg.* **2017**, *27*, 288–294. [CrossRef] [PubMed]
22. Ferrannini, E.; Mingrone, G. Impact of different bariatric surgical procedures on insulin action and beta-cell function in type 2 diabetes. *Diabetes Care* **2009**, *32*, 514–520. [CrossRef] [PubMed]
23. Schwartz, M.W.; Boyko, E.J.; Kahn, S.E.; Ravussin, E.; Bogardus, C. Reduced insulin secretion: An independent predictor of body weight gain. *J. Clin. Endocrinol. Metab.* **1995**, *80*, 1571–1576. [CrossRef] [PubMed]
24. Lee, Y.H.; Magkos, F.; Mantzoros, C.S.; Kang, E.S. Effects of leptin and adiponectin on pancreatic β-cell function. *Metabolism* **2011**, *60*, 1664–1672. [CrossRef]
25. Biondi, G.; Marrano, N.; Borrelli, A.; Rella, M.; Palma, G.; Calderoni, I.; Siciliano, E.; Lops, P.; Giorgino, F.; Natalicchio, A. Adipose Tissue Secretion Pattern Influences β-Cell Wellness in the Transition from Obesity to Type 2 Diabetes. *Int. J. Mol. Sci.* **2022**, *23*, 5522. [CrossRef]
26. Han, Y.; Sun, Q.; Chen, W.; Gao, Y.; Ye, J.; Chen, Y.; Wang, T.; Gao, L.; Liu, Y.; Yang, Y. New advances of adiponectin in regulating obesity and related metabolic syndromes. *J. Pharm. Anal.* **2024**, *14*, 100913. [CrossRef]
27. Ma, W.; Huang, T.; Zheng, Y.; Wang, M.; Bray, G.A.; Sacks, F.M.; Qi, L. Weight-Loss Diets, Adiponectin, and Changes in Cardiometabolic Risk in the 2-Year POUNDS Lost Trial. *J. Clin. Endocrinol. Metab.* **2016**, *101*, 2415–2422. [CrossRef]
28. Nelalcazar, L.M.; Lang, W.; Haffner, S.M.; Schwenke, D.C.; Kriska, A.; Balasubramanyam, A.; Hoogeveen, R.C.; Pi-Sunyer, F.X.; Tracy, R.P.; Ballantyne, C.M. and Look AHEAD (Action for Health in Diabetes) Research Group. Improving Adiponectin Levels in Individuals With Diabetes and Obesity: Insights From Look AHEAD. *Diabetes Care* **2015**, *38*, 1544–1550. [CrossRef]
29. Allin, K.H.; Friedrich, N.; Pietzner, M.; Grarup, N.; Thuesen, B.H.; Linneberg, A.; Pisinger, C.; Hansen, T.; Pedersen, O.; Sandholt, C.H. Genetic determinants of serum vitamin B12 and their relation to body mass index. *Eur. J. Epidemiol.* **2017**, *32*, 125–134. [CrossRef]
30. Gunanti, I.R.; Marks, G.C.; Al-Mamun, A.; Long, K.Z. Low serum vitamin B-12 and folate concentrations and low thiamin and riboflavin intakes are inversely associated with greater adiposity in Mexican American children. *J. Nutr.* **2014**, *144*, 2027–2033. [CrossRef]
31. Kumar, K.A.; Lalitha, A.; Pavithra, D.; Padmavathi, I.J.; Ganeshan, M.; Rao, K.R.; Venu, L.; Balakrishna, N.; Shanker, N.H.; Reddy, S.U.; et al. Maternal dietary folate and/or vitamin B12 restrictions alter body composition (adiposity) and lipid metabolism in Wistar rat offspring. *J. Nutr. Biochem.* **2013**, *24*, 25–31. [CrossRef] [PubMed]
32. Adaikalakoteswari, A.; Finer, S.; Voyias, P.D.; McCarthy, C.M.; Vatish, M.; Moore, J.; Smart-Halajko, M.; Bawazeer, N.; Al-Daghri, N.M.; McTernan, P.G.; et al. Vitamin B_{12} insufficiency induces cholesterol biosynthesis by limiting s-adenosylmethionine and modulating the methylation of SREBF1 and LDLR genes. *Clin. Epigenetics* **2015**, *7*, 14. [CrossRef] [PubMed]
33. Sun, W.L.; Hua, S.; Li, X.Y.; Shen, L.; Wu, H.; Ji, H.F. Microbially produced vitamin B12 contributes to the lipid-lowering effect of silymarin. *Nat. Commun.* **2023**, *14*, 477. [CrossRef] [PubMed]
34. Dadson, P.; Rebelos, E.; Honka, H.; Juárez-Orozco, L.E.; Kalliokoski, K.K.; Iozzo, P.; Teuho, J.; Salminen, P.; Pihlajamäki, J.; Hannukainen, J.C.; et al. Change in abdominal, but not femoral subcutaneous fat CT-radiodensity is associated with improved metabolic profile after bariatric surgery. *Nutr. Metab. Cardiovasc. Dis.* **2020**, *30*, 2363–2371. [CrossRef]
35. Ebadi, M.; Dunichand-Hoedl, A.R.; Rider, E.; Kneteman, N.M.; Shapiro, J.; Bigam, D.; Dajani, K.; Mazurak, V.C.; Baracos, V.E.; Montano-Loza, A.J. Higher subcutaneous adipose tissue radiodensity is associated with increased mortality in patients with cirrhosis. *JHEP Rep.* **2022**, *4*, 100495. [CrossRef]